Molecular Organization and Motions of Cholesteryl Esters in Crystalline and Liquid Crystalline Phases: A ^{13}C and ^{1}H Magic Angle Spinning NMR Study†

Wen Guo and James A. Hamilton*

Biophysics Department, Housman Medical Research Center, Boston University School of Medicine, 80 East Concord Street Boston, Massachusetts 02118-2394

Received March 31, 1993; Revised Manuscript Received June 11, 1993

ABSTRACT: Cholesteryl esters are a major lipid constitutent of plasma lipoproteins and atherosclerotic lesions. Crystalline and liquid crystalline phases of several cholesteryl esters [oleate (C18:1, ω-9), erucate (C22:1, ω-9), hexanoate (C6:0), decanoate (C10:0), undecanoate (C11:0), myristate (C14:0), palmitate (C16:0), and stearate (C18:0)] have been studied by natural abundance ^{13}C NMR with magic angle spinning (MASNMR) at 75 MHz (7.05 T). Spectra obtained with magic angle spinning, high-power proton decoupling, and cross-polarization transfer were highly resolved for crystalline cholesteryl esters. Acyl chain carbons had narrower lines than protonated steroid ring carbons, reflecting differential motions in the crystal (specifically, more rapid motions in the acyl chain than in the steroid ring). Esters which crystallize into the monolayer type II structure, in which all molecules are equivalent, gave rise to a single resonance for each carbon; esters of the monolayer type I and bilayer structures, in which there are two types of nonequivalent molecules in the unit cell, had two resonances (equal intensity and line width) for several carbons, such as the carbonyl and the steroid ring C5 and C6. Spectra for liquid crystalline phases did not show inequivalence of signals for the same carbon and were not enhanced by cross-polarization transfer. These changes are a result of increased molecular motions in the liquid crystals, which average the nonequivalent environments and reduce the dipolar interactions. Cholesteric and smectic liquid crystalline phases were distinguished by the broader C=O, C5, and C6 signals for the cholesteric compared with the smectic phase. In the smectic phase, chemical shifts of corresponding carbons of all cholesteryl esters are similar and are close to those for crystalline esters with a monolayer II structure, which suggests that the smectic phase has structural features resembling the monolayer II crystal structure. ^{13}C MASNMR is thus a powerful approach for examining structure and motions of crystalline and liquid-crystalline cholesteryl esters. ^{1}H MASNMR spectra did not give as detailed information on the molecular level but were unique for each phase and provided a simple and quick method for distinguishing the solid, smectic, cholesteric, and isotropic phases.

Cholesteryl esters serve as a transport and storage form of cholesterol in mammals (Brown & Goldstein, 1986; Jones & Glomset, 1985). They also constitute a major fraction of the lipids present in atherosclerotic plaques (Small, 1988). Because they are weakly polar molecules, cholesteryl esters have a very low solubility in phospholipid interfaces (Gorrissen et al., 1980; Hamilton et al., 1982, 1983) and form separate phases, which can consist of pure or nearly pure cholesteryl esters. A thorough understanding of the aggregation properties of pure cholesteryl esters in various physical states is therefore important in both normal and pathophysiology.

The polymorphism and mesomorphism of cholesteryl esters have been extensively studied by different physical methods such as differential scanning calorimetry (Davis et al., 1970), X-ray diffraction (Craven, 1986; Gao & Craven, 1986), electron diffraction (Dorset, 1985), polarizing microscopy (Gray, 1962), and nuclear magnetic resonance (NMR)[1] spectroscopy (Hamilton et al., 1977; Kroon, 1981; Ginsburg et al., 1982; Croll et al., 1985, 1986). Although microscopy and calorimetry are informative and convenient methods for the study of phase transition behavior, they usually provide little knowledge on the molecular level. Single-crystal X-ray diffraction can give a three-dimensional molecular structure in the crystalline phase; however, information is limited to the crystalline state, and the requirement for appropriate single crystals often limits its application.

Compared with these methods, NMR spectroscopy is remarkable for its ability to observe each segment of a molecule in any physical state. Molecular arrangements in different phases can be detected by the chemical shift, and molecular motions by relaxation time measurements or orientational ordering parameters. High-resolution ^{13}C NMR spectroscopy has provided details about the molecular motions and intermolecular interactions of cholesteryl esters in liquid and liquid crystalline phases (Hamilton et al., 1977; Ginsburg et al., 1982; Croll & Hamilton, 1986). However, the characterization of mesophases was limited by extensive line broadening and the consequent loss of spectral information, and no spectral information was obtained from crystalline cholesteryl esters. The orientational ordering of cholesteryl esters in mesophases can be studied by ^{2}H NMR spectroscopy but requires either perdeuteration or single site deuteration, which is positional specific and less perturbing, but which entails a more difficult synthetic protocol (Luz et al., 1981).

The technique of NMR with magic angle sample spinning (MASNMR) can potentially eliminate the extensive line broadening in ^{13}C spectra of ordered/anisotropic systems and yield high-resolution spectra from which chemical shift and relaxation measurements can be made. This method is newer than high-resolution spectroscopy of liquids and has seen

† Supported by RO1 HL41904.

* To whom correspondence should be addressed.

[1] Abbreviations: NMR, nuclear magnetic resonance, MAS, magic angle spinning, CP, cross-polarization transfer; HP, high power proton decoupling; SSB, spinning side bands; CSA, chemical shift anisotropy; Am, amorphous phase; Cr, crystalline phase; Iso, isotropic phase; *MLII*, monolayer II; *MLI*, monolayer I; Sm, smectic phase; Ch*, cholesteric phase.

0006-2960/93/0432-9038$04.00/0

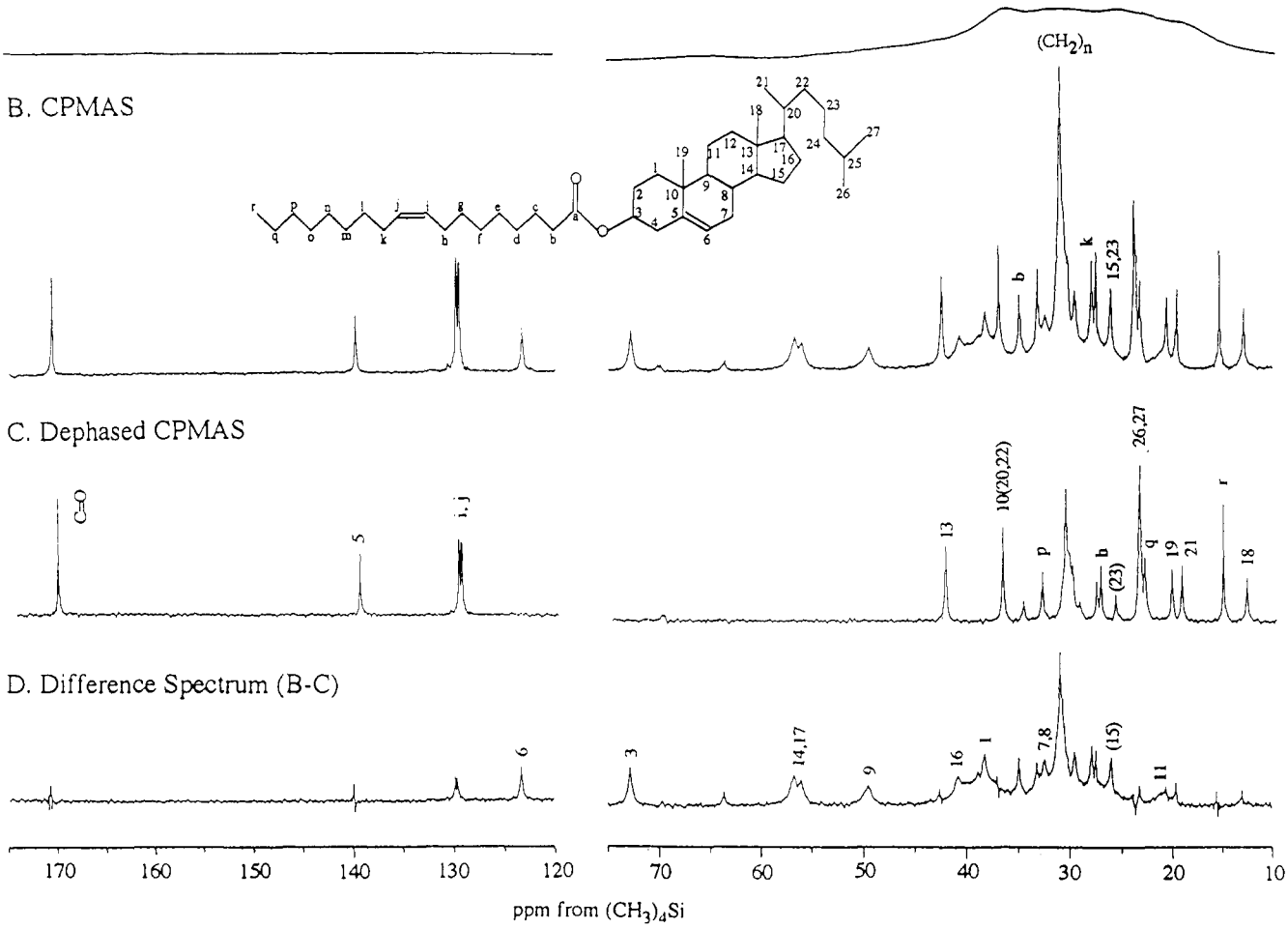

FIGURE 1: ^{13}C NMR spectra at 75 MHz and 25 °C of crystalline cholesteryl oleate. (A) Standard CP spectrum with a nonspinning sample; (B) standard CP spectrum with MAS; (C) dephased CP spectrum with MAS and a 50-μs delay inserted between the CP contact pulse and the data acquisition; (D) difference spectrum of B and C. Peaks are designated by the carbon number for the cholesteryl moiety and by letters for the acyl chain (inset). Peaks in parentheses are probable, but not certain, assignments. Peaks labeled in B are seen in both C and D and may represent two nuclei with different mobility or a single nucleus with an intermediate mobility; peaks labeled in C have lost little intensity and reflect slower relaxing nuclei (i.e., those with greater mobility). *Note that the nonprotonated C=O, C5, C13, and C10 are among the rigid group.* Peaks labeled in D are those which do not appear at all in the dephased spectrum and reflect the nuclei with strong dipolar relaxation (rigid protonated carbon nuclei). Spectra B and C were obtained with a spinning rate of 4.5 kHz. Spectra were processed without line broadening (as in the following figures unless otherwise indicated) after 10 000 scans (A) and 1000 scans (B and C).

limited application to liquid crystalline model membranes and biological membranes (Griffin, 1981; Forbes et al., 1988; Jacobs & Oldfield, 1981; Oldfield et al., 1987, 1991) and crystalline lipids (Bociek et al., 1985; Norton et al., 1985; Webb & Zilm, 1989; Byrn et al., 1988).

In the present work, we report a systematic investigation of eight different cholesteryl esters. With the combination of solid-state MAS and cross-polarization transfer (CPMAS) natural abundance ^{13}C NMR spectroscopy, we examined three different typical crystalline forms and cholesteric and smectic mesophases. Well-resolved ^{13}C spectra with numerous single carbon resonances were obtained for all phases and yielded quantitative information about molecular structures and motions. ^{1}H MASNMR spectra did not exhibit as high resolution in the anisotropic phases as the ^{13}C spectra but were characteristic of each particular phase.

EXPERIMENTAL PROCEDURES

Cholesteryl esters (>99%) were purchased from Nu-chek company (Elysian, MN) and used without further purification. Thin-layer chromatography of the esters in 96:4:1 hexane–diethyl ether–acetic acid showed a single spot (Ginsburg et al., 1982). All NMR measurements were performed on a Bruker AMX-300 (7.05 T, corresponding to 75 MHz for ^{13}C) equipped with a BL-7 magic angle spinning probe and a high-power amplifier unit. Samples were placed in a 7-mm ZrO_2 rotor (~400-μL sample volume) with or without a "cramps" insert made with Kel-F material. The use of such inserts reduces the sample size to a small spherical volume (~150 μL) and improves the field homogeneity of the sample and enables smooth spinning at high rates. Sample spinning rates were 4.5 kHz for solid states and 2–4 kHz for mesophases and isotropic phases. Typical decoupling power was about 55 W for solid states, 25 W for mesophases, and 15 W for the isotropic phase. To minimize the rf heating effect, a duty cycle of $\leq$1% was used for all experiments. For crystalline samples, single-contact cross-polarization from the ^{1}H reservoir to ^{13}C spins was employed to increase the ^{13}C sensitivity and shorten the effective ^{13}C relaxation time (Fyfe, 1983). The typical spin-lock field was about 50 kHz, and, unless otherwise indicated, the typical CP contact time was 5 ms and the pulse interval 7.0 s. For liquid crystalline and isotropic states, a standard single 90° (5-μs) pulse ^{1}H-decoupled ^{13}C MASNMR experiment which uses high-power decoupling (HP) without CP

Table I: Values of the ^{13}C Chemical Shifts (ppm) of Crystalline Cholesteryl Esters

	monolayer II			monolayer I		bilayer		
peak assignment	C18:1	C22:1	C6:0	C10:0	C11:0	C14:0	C16:0	C18:0
C=O	170.76	170.72	171.39	182.93 170.89	173.05 B 171.46 A	170.97 170.60	170.97 170.59	170.98 BL 170.59 AL
C5	139.92	139.66	140.28	141.00 140.69	140.93 A 140.58 B	142.32 141.88	142.33 141.88	142.33 A 141.88 B
C=C	129.80 129.54	129.93 129.31						
C6	123.31	123.23	122.94	122.89 121.31	122.98 A 121.52 B	120.72 120.15 B	120.72 120.14	120.71 A 120.13 B
C3	72.80	72.29	72.71	74.77 72.70	74.79 B 72.71 A	71.52	71.49	71.48
C14,17	56.76 56.04	56.64 55.83	56.73 56.36	57.57 56.08	57.67 56.12	57.85 56.68	57.85 56.72	57.83 56.87
C9	49.52	49.43	49.50	50.72 50.20	50.75 A 50.35 B	49.77	49.53	49.74
C13	42.46	42.36	42.31	42.54	42.53	42.87 42.59	42.88 42.58	42.88 B 42.59 A
C16	40.78	40.42	40.85	41.01	41.05	40.38	40.38	40.37
C24	*a*	*a*	*a*	40.09	40.69	40.38	40.38	40.37
C4	*a*	*a*	39.20	38.04	38.52	38.93	38.95	38.94
C1	38.30	38.14	38.05	38.04	37.94	38.42	38.39	38.38
C10,20,22 C10	36.98	36.91	36.85	36.57	36.52	37.17 37.00	37.21 37.00	37.20 A 37.01 B
bCH_2	34.95	34.83	34.74	*a*	*a*	34.80	34.74	34.79
$(\omega\text{-}2)CH_2$; C7,8	32.46	32.95	32.48	32.13	32.35	*a*	*a*	*a*
$(CH2)_n$	30.95	31.62		30.73	30.53	32.53	32.42	32.55
C12,25	29.61	29.43	29.42	29.07	29.13	27.78	27.79	27.80
CC=C	27.98 27.57	27.90 27.48						
C26,27	23.78	23.98	23.81	24.10	24.43	22.89	23.17	22.89
$(\omega\text{-}1)CH_2$	23.29	23.02	22.83	23.37	23.37	22.40	22.91	22.39
C19	20.65	20.68	19.85	20.68 20.46	21.04 20.19	19.38 18.97	19.40 18.97	19.39 A 18.98 B
C21	19.64	19.38	19.85	19.93 19.69	19.80 19.40	18.97	18.97	18.98
$\omega\text{-}CH_3$	15.44	15.17	14.55	15.03	15.78 A 14.25 B	15.34 14.82	15.33 14.82	15.34 BL 14.81 AL
C18	13.01	12.88	12.92	12.27 11.98	12.02	13.55 11.75	13.56 11.75	13.51 B 11.76 A

[a] These peaks are buried under the broad superimposed peak and could not be resolved accurately.

was used. For the isotropic phase and stable liquid crystalline phases, the pulse interval was typically 7.0 s, whereas for metastable liquid crystalline phases, a recycle time of 1–2 s was used to minimize the total experimental time (to avoid solidification from the liquid crystal phase). The ^{13}C chemical shifts were all referred to the carbonyl carbon peak of glycine [176.06 ppm from $(CH_3)_4Si$] as an external reference. Peak assignments were made on the basis of the assignment of cholesteryl esters in the isotropic state (Hamilton et al., 1977; Ginsburg et al., 1982). Spectra were typically obtained over 2K time domain points and zero-filled to 16K, giving a spectral digital resolution of about 1.0 Hz. Sample temperatures were controlled to within 1 °C with the Bruker B-VT-1000 variable temperature unit. Samples were allowed to equilibrate at the desired temperature for 15–20 min before data acquisition on stable phases and a shorter time for metastable phases. The actual probe temperature was calibrated by observing the correlating the changes in the ^{13}C MASNMR spectrum with the known phase transition temperatures of pure cholesteryl esters (Ginsburg et al., 1984).

^{13}C spin–lattice relaxation times (T_1) in the crystalline phase were measured with a modified inversion–recovery pulse sequence with signal enhancement by CP (Torchia, 1978). Pre-acquisition delays of 15 and 180 s were used for the carbon nuclei with short T_1 and long T_1 values, respectively. For liquid crystalline and isotropic phases, a standard inversion–recovery pulse sequence was used with a pre-acquisition delay of 15 s. The observed signal intensities were fit with a three-parameter equation to yield the T_1 values.

RESULTS

^{13}C MASNMR Spectra of Cholesteryl Esters in the Crystalline State

Three general molecular packing arrangements for cholesteryl esters with different fatty acid chains have been characterized by single-crystal X-ray crystallography: monolayer type I (*MLI*), monolayer type II (*MLII*), and bilayer (Craven, 1986). In the present work, crystalline forms of six saturated and two monounsaturated cholesteryl esters have been studied. They belong to (i) *MLII*, including oleoyl (C18:

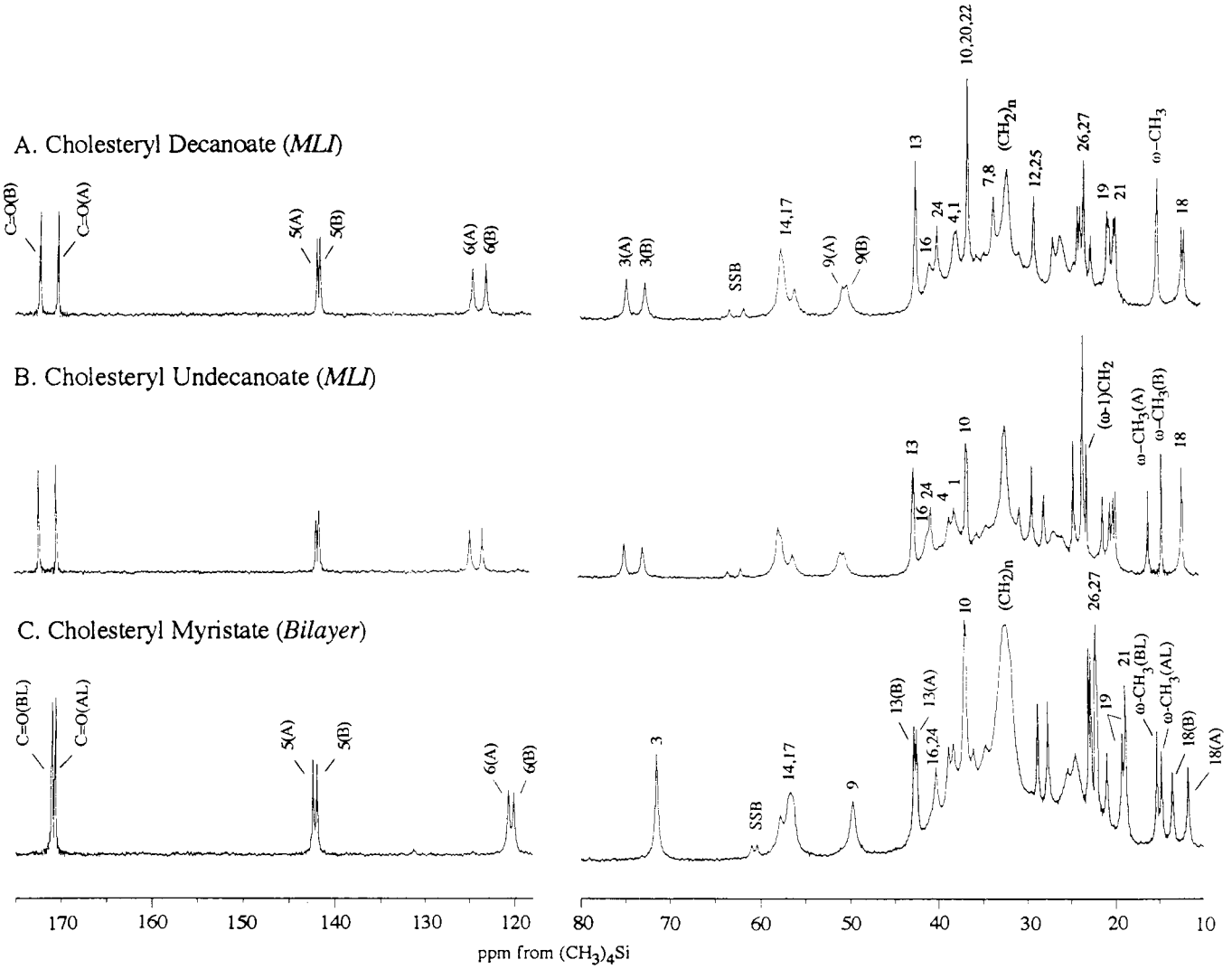

FIGURE 2: ^{13}C MASNMR spectra at 25 °C of crystalline (A) cholesteryl decanoate, (B) cholesteryl undecanoate, and (C) cholesteryl myristate. All spectra were acquired with a standard CP pulse sequence and a spinning rate of 4.5 kHz with 1000 scans. Peaks for the cholesteryl moiety are designated by the carbon number; ω-CH_3, (ω-1)CH_2, and $(CH_2)_n$ identify the terminal methyl, the terminal CH_2, and the bulk methylene carbons of the acyl chain, respectively. Among the resonances that are not readily assigned in the complex aliphatic regions are those for the acyl $\underline{C}H_2CO$ and $\underline{C}H_2CH_2CO$.

1, ω-9), erucyl (C22:1, ω-9), and hexanoyl (C6:0); (ii) *MLI*, including decanoyl (C10:0) and undecanoyl (C11:0); and (iii) bilayer, including myristoyl (C14:0), palmitoyl (C16:0), and stearoyl (C18:0).

Monolayer Type II. Solid-state ^{13}C NMR spectra at 25 °C of the biologically abundant cholesteryl ester cholesteryl oleate are shown in Figure 1. The spectrum acquired with a single-contact CP pulse sequence and HP on a *nonspinning* sample (Figure 1A) shows only broad featureless signals, as expected, and provides no information about single carbons in the molecule. In contrast, under conditions of MAS, HP, and CP, the crystalline sample shows a highly resolved spectrum with numerous narrow single-carbon resonances. Resolution is comparable to that for the isotropic liquid phase; remarkably, the spectrum of the crystalline phase shows a pattern of differential line broadening (Figure 1B) very much like the liquid state (Hamilton et al., 1977; Ginsburg et al., 1982; Figures 4C and 6F). Notably, resonances from protonated carbons of the steroid ring are significantly broader than resonances for nonprotonated ring carbons and carbons of the acyl and isooctyl side chains.

A possible explanation for differential line broadening is that there are different frequencies of motion in crystalline cholesteryl oleate, which are detected by NMR. To test this hypothesis, a dipolar dephasing pulse sequence was used, in which a short delay (50 μs) was inserted between the CP contact and the data acquisition. The delay permits decay of signals from carbon nuclei with the strongest dipolar coupling interactions (the most rigid protonated carbons) and has little effect on signals of protonated carbons with less restricted motions or on signals of nonprotonated carbons (Bociek et al., 1985). The MASNMR spectrum of cholesteryl oleate after dephasing (Figure 1C) shows signals for the C=O, the nonprotonated carbons C5, C13, and C10, the angular methyls C18 and C19, the side chain methyls C26 and C27, and several acyl chain carbons. The protonated carbons seen in this spectrum are relatively mobile and correspond to those carbons which are poorly resolved in the crystal structure (Craven, 1986). The difference spectrum (Figure 1D) shows the broader peaks of the more rigid carbons (e.g., the C6, C3, C14, 17, C9, and C4) which were selectively removed from the dephased CPMAS spectrum. T_1 measurements for crystalline cholesteryl erucate (*MLII*) provide additional evidence for differential motions in the crystalline esters (see below).

The ^{13}C MASNMR spectra of crystalline cholesteryl hexaonate (not shown) and erucate (see below, Figure 4A) had the same features as cholesteryl oleate (except that the hexanoate ester gives no olefinyl signals). Therefore, the spectra of cholesteryl oleate shown in Figure 1 are represen-

Table II: Values of the ^{13}C Chemical Shifts (ppm) of Cholesteryl Esters in the Noncrystalline Phases

	eurcyl		oleoyl			myristyl		
peak assignment	Sm	I	Sm	Ch*	I	Sm	Ch*	I
C=O	171.0	171.0	170.1	171.1	171.1	171.3	171.3	171.3
C5	139.9	139.9	139.9	139.8	140.0	140.2	140.2	140.1
C=C	129.6	129.7	129.6	129.7	129.7			
C6	122.3	122.3	122.4	122.3	122.3	122.4	122.4	122.3
C3	73.1	73.0	73.1	73.0	73.1	73.4	73.4	73.3
C14,17	56.9, 56.7	56.8	56.8	56.7	56.8	57.2, 56.9	57.1	57.0
C9	50.0	50.2	50.0	50.1	50.2	50.3	50.3	50.4
C13	42.5	42.5	42.5	42.4	42.5	42.8	42.7	42.7
C16	40.1	40.0	40.1	39.7	39.8	40.3	40.3	40.2
C24	39.8	39.7	39.8	39.7	39.7	39.9	39.9	39.8
C4	38.4	38.5	38.5	38.5	38.5	38.5	38.7	38.6
C1	37.2	37.2	37.2	37.4	37.4	37.5	37.4	37.3
C10,20,22	36.7	36.7	36.7	36.6	36.7	37.0	36.9	36.8
bCH_2	34.6	34.4	34.8	34.7	34.6	34.5	34.4	34.4
$(\omega\text{-}2)CH_2$; C7,8	32.1	32.1	32.2	32.1	32.2	32.3	32.3	32.2
$(CH2)_n$	29.5	29.6	30.0	29.5	29.6	30.4	29.8	29.7
	30.4	29.9	29.6	29.8	29.9		30.2	30.0
C2	28.5	28.4	28.7	28.6	28.5	28.7	28.5	28.4
C12,25	28.2	28.1	28.2	28.1	28.1	28.3	28.2	28.1
C - C=C	27.3	27.3	27.4	27.3	27.3			
	27.3	27.3	27.4	27.3	27.3			
C15	25.3	25.1	25.3	25.1	25.1	25.4	25.3	25.2
C23	24.5	24.5	24.6	24.6	24.6	25.1	24.9	24.6
$(\omega\text{-}1)CH_2$; C26,27	22.8	22.8	22.8	22.7	22.7	22.9	22.8	22.8
C11	21.3	21.3	21.4	21.4	21.4	21.5	21.4	21.4
C19	19.5	19.4	19.6	19.4	19.4	19.7	19.6	19.5
C21	19.0	19.0	19.0	19.0	19.0	19.2	19.1	19.1
$\omega\text{-}CH_3$	14.1	14.1	14.2	14.1	14.1	14.1	14.1	14.1
C18	12.1	12.0	12.1	12.0	12.0	12.3	12.2	12.1

tative of these esters in the crystalline state. Table I summarizes the assignments and chemical shifts for these MLII esters.

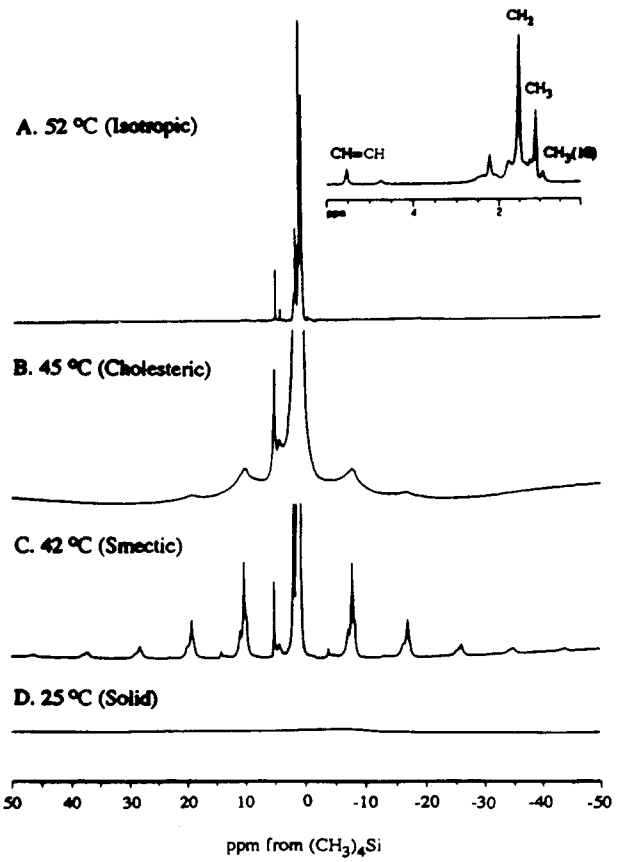

FIGURE 3: ^1H MASNMR spectra at 300 MHz of cholesteryl oleate in (A) the isotropic liquid phase (52 °C) (inset is an expansion of the 0–6 ppm region); (B) the cholesteric phase (45 °C); (C) the smectic phase (42 °C); and (D) the crystalline phase (25 °C). Samples were spun at 3 kHz at the magic angle.

Monolayer Type I. The ^{13}C MASNMR spectra at 25 °C of two cholesteryl esters [cholesteryl decanoate (C10:0) and undecanoate (C11:0)] belonging to *MLII* are shown in Figure 2 panels A and B, respectively. Compared with spectra of *MLII* crystals, the most significant difference is that there are two distinct sets of resonances with equal intensities for carbon nuclei at a few specific positions, most notably the C=O, C5, C6, C3, and C9. As shown in Table I, the two sets of peaks for C=O, C6, and C3 are separated by 1.5–2.0 ppm, and those for C5 and C9 by ~0.4 ppm. These separations are about the same for both C10:0 and C11:0 esters. The two sets of peaks are attributed to the nonequivalent A and B molecules in the *MLI* crystal lattice (see Discussion). There are also sets of nonequivalent resonances in the aliphatic region (10–40 ppm) for some methyl and methylene carbons such as the C18, ω-CH_3, C19, and C21. This region is less well resolved for *MLI* than for *MLII* crystals (Figure 1B) probably because of additional peak multiplicities, although these cannot be clearly assigned. The two sets of peaks are attributed to the nonequivalent A and B molecules in the *MLI* crystalline lattice (see Discussion).

Bilayer. Cholesteryl esters which crystallize into a bilayer structure also consist of molecules A and B, which are not related by crystal symmetry. This group includes the long saturated chain series cholesteryl myristate (C14:0), palmitate (C16:0), and stearate (C18:0). The ^{13}C MASNMR spectra of esters in this group were quite similar, and only that of C14:0 is shown (Figure 2C). Values of the chemical shift for all three esters are listed in Table II. From Figure 2C and Table II, it is clear that there are two distinct sets of resonances for C=O, C5, C6, C13, C10, C18, and the ω-CH_3, as in the case of MLI crystals (Figure 2A,B), but the peak separations are comparatively small (<0.5 ppm), except for the C18 signals (1.8 ppm). In contrast to *MLI* crystals, the bilayer crystals show a single signal for C3 and C9.

^1H and ^{13}C MASNMR Spectra of Liquid and Liquid Crystalline Phases Cholesteryl esters form either stable mesophases, which form as the crystal melts, or metastable

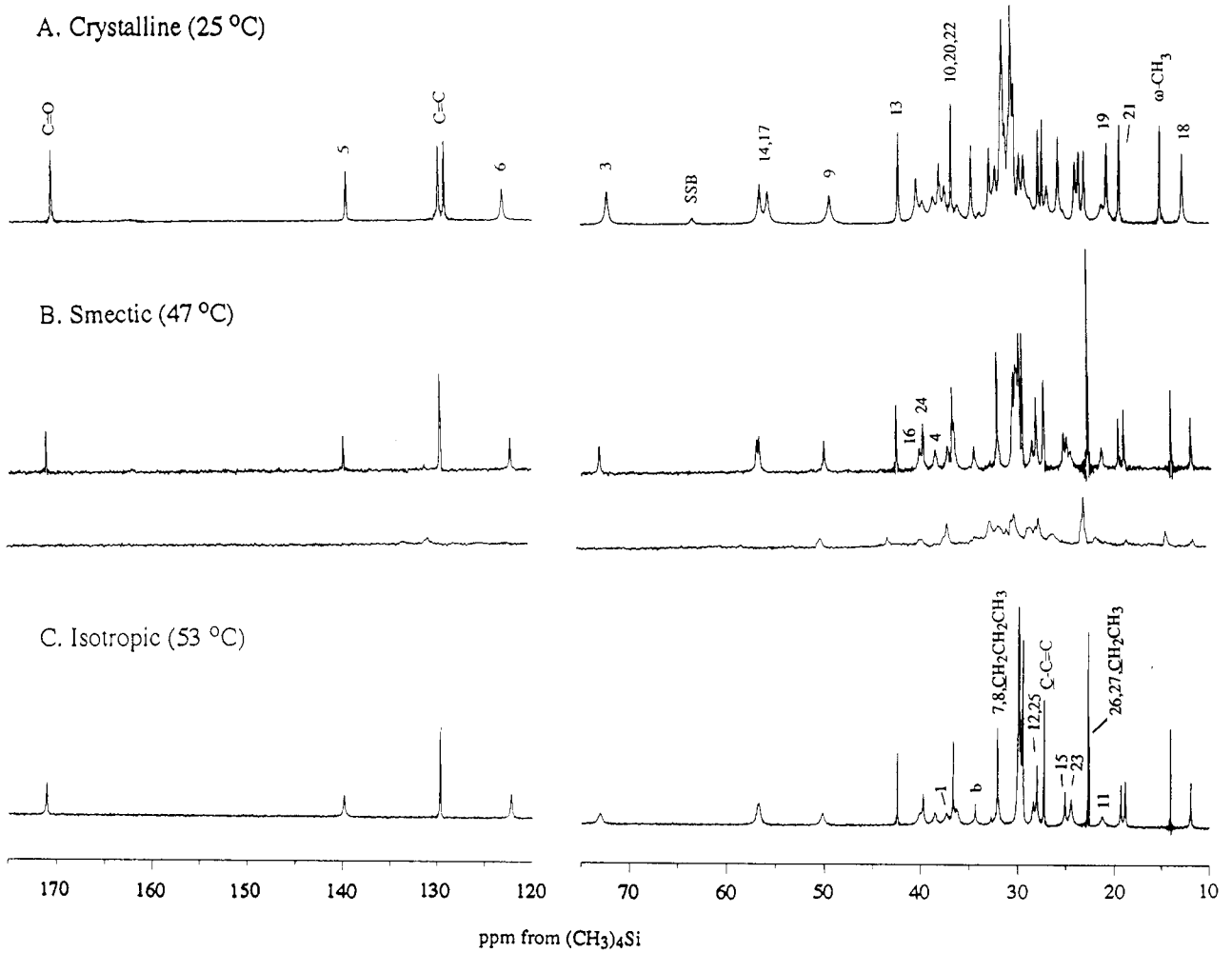

FIGURE 4: ^{13}C MASNMR spectra of cholesteryl erucate in (A) the crystalline phase (25 °C), MAS spinning rate = 4.5 kHz; (B) the smectic phase (47 °C), MAS spinning rate = 3.0 kHz. The spectrum in the inset was taken at the same temperature, but the sample spinning axis was changed to 47°, about 7° off the magic angle; the sample was spun at 500 Hz. (C) The isotropic liquid phase (53 °C), MAS spinning rate = 3.0 kHz.

mesophases, which form at temperatures below the crystal melting temperature. We used ^1H and ^{13}C MASNMR to study the mesophases of three cholesteryl esters (C14:0, C22:1, and C18:1), among which C14:0 and C22:1 form stable, and C18:1 forms metastable, mesophases.

The ^1H MASNMR spectra corresponding to isotropic, cholesteric, smectic, and crystalline phases of cholesteryl oleate (C18:1) are shown in Figure 3, panels A–D, respectively. The spectrum of the isotropic phase is characterized by high-resolution features, comparable to those of conventional high-resolution ^1H spectra (Kroon, 1981). Further increases in temperature do not cause significant changes in such a proton spectrum, which confirms that the sample is completely melted. When the sample is cooled to the isotropic–cholesteric phase transition temperature, the ^1H spectrum changes abruptly into a pattern (Figure 3B) characterized by a much broader center peak flanked by broad spinning side bands. Further temperature decreases in the range corresponding to that of the cholesteric phase cause only slight changes in the sideband intensities. At the cholesteric–smectic phase transition temperature, the ^1H spectrum changes abruptly into a pattern (Figure 3C) characterized by a rather narrow center peak flanked by its spinning side bands. This pattern is temperature independent as long as the sample remains in the smectic phase. For cholesteryl oleate, solidification started soon after cooling to ~25 °C or after extended incubation of either the cholesteric or smectic liquid crystalline phase at higher temperatures. In all cases the solidification was characterized by the appearance of an extremely broad and featureless signal below the relatively sharp peaks of the residual mobile phases. When the solidification was complete, the ^1H spectrum (Figure 3D) became extremely broad.

The same spectral changes accompany the phase transitions of the two other cholesteryl esters investigated (erucate and myristate) and provide a very sensitive and reliable method to identify the phase of cholesteryl esters by ^1H NMR. Furthermore, a *quick* assessment of the physical state of the cholesteryl esters can be made, since the ^1H spectrum requires only one scan (a few seconds).

^{13}C MASNMR spectra are also unique for each phase of cholesteryl esters, but the differences are less dramatic than those of ^1H spectra. The ^{13}C spectra of cholesteryl erucate (C22:1) in the *MLII* crystalline, smectic, and isotropic phase are shown in Figure 4, panels A–C, respectively. The spectrum of the crystalline ester was obtained with CP, whereas those for the noncrystalline states were obtained with HP only. Comparison of Figure 4 panels A and B shows that all peaks in the ^{13}C spectrum of the smectic phase are somewhat narrower than those of the crystalline phase; consequently the crowded aliphatic region (10–40 ppm) is better resolved for the smectic (Figure 4B) compared to crystalline phase (Figure 4A). In addition, some small differences are found in the chemical shift values for corresponding carbons in the smectic and crystalline spectra (Tables I and II). Another way to distinguish crystalline and smectic phases is that the smectic phase does not show significant signal enhancement with CP

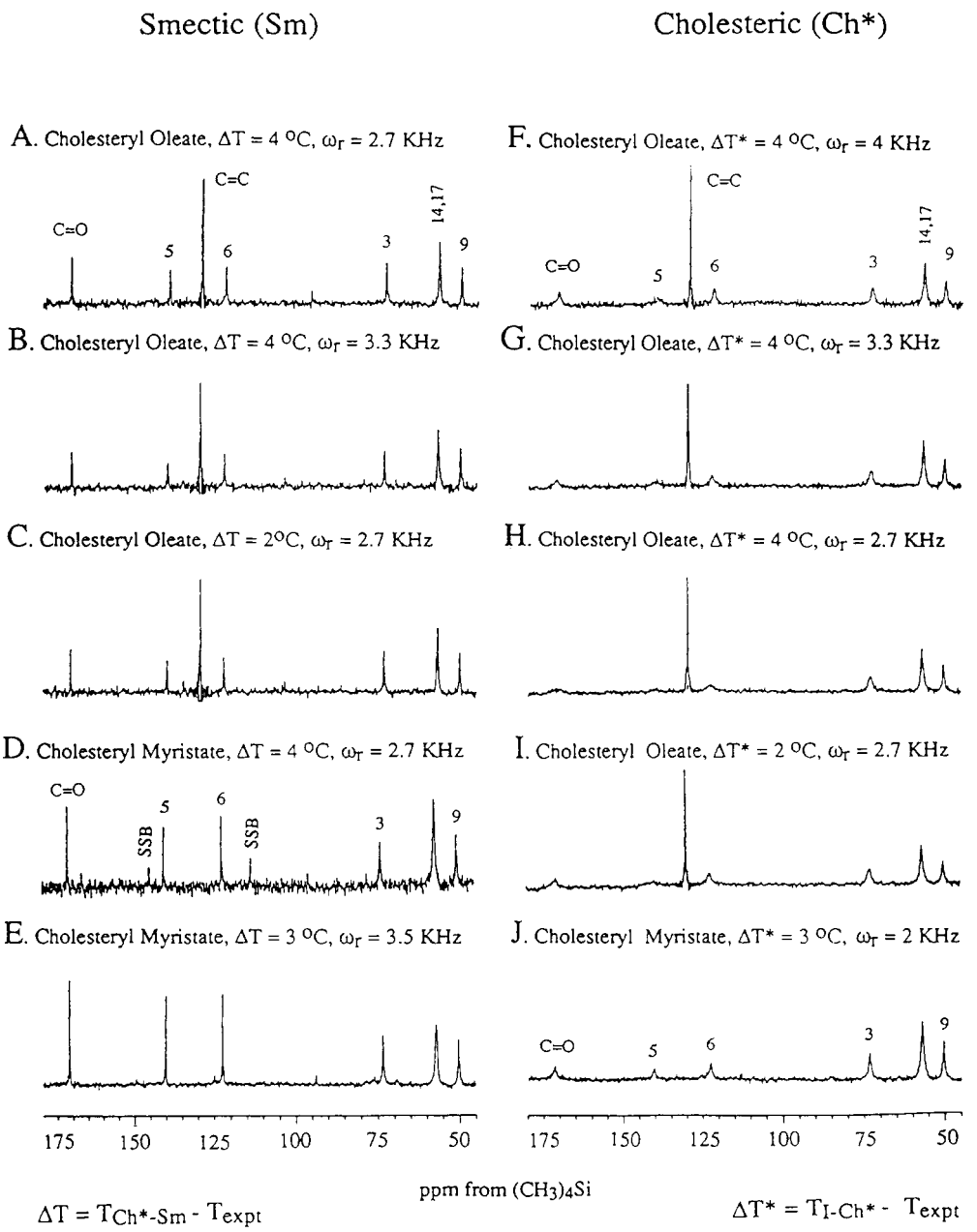

FIGURE 5: ^{13}MASNMR spectra of liquid crystalline cholesteryl esters at different temperatures and MAS spinning rates. Spectra of the smectic phases were processed without line broadening; spectra of the cholesteric phases were processed with 5 Hz line broadening. All spectra were obtained with 1000 scans. (A) Cholesteryl oleate, smectic (Sm) phase, at 4 °C below the cholesteric to smectic phase transition temperature (ΔT = 4 °C), spinning rate (ω_r) = 2.7 kHz; (B) cholesteryl oleate, Sm, ΔT = 4 °C, ω_r = 3.3 kHz; (C) cholesteryl oleate, Sm, ΔT = 2 °C, ω_r = 2.7 kHz; (D) cholesteryl myristate, Sm, ΔT = 4 °C, ω_r = 2.7 kHz; (E) cholesteryl myristate, Sm, ΔT = 3 °C, ω_r = 3.5 kHz; (F) cholesteryl oleate, cholesteric phase (Ch*), at 4 °C below the isotropic to cholesteric phase transition temperature (ΔT^* = 4 °C), ω_r = 4.0 kHz; (G) cholesteryl oleate, Ch*, ΔT^* = 4 °C, ω_r = 3.3 kHz; (H) cholesteryl oleate, Ch*, ΔT^* = 4 °C, ω_r = 2.7 kHz; (I) cholesteryl oleate, Ch*, ΔT^* = 2 °C, ω_r = 2.7 kHz; (J) cholesteryl myristate, Ch*, ΔT^* = 3 °C, ω_r = 2.0 kHz.

(spectrum not shown) compared to single-pulse ^{13}C MAS-NMR with HP only (Figure 4B) because increased thermal motion in the liquid crystalline phase reduces H–C dipolar interactions considerably.

Cholesteryl erucate does not form a cholesteric phase, and the general features of the ^{13}C MASNMR spectrum of the smectic phase (Figure 4B) are quite similar to those of the isotropic phase (Figure 4C). These two phases, however, can be differentiated by the following: (i) The smectic phase usually gives spinning side bands for the unsaturated carbons (e.g., C=O, C5, C6), which have larger chemical shift anisotropies than the saturated carbons (such an effect is more readily observed at lower MAS rate, e.g., 1–2 kHz). The isotropic phase does not exhibit spinning side bands since the chemical shift anisotropy (CSA) is averaged to zero for all the carbons. (ii) With off-magic angle spinning, the isotropic phase still exhibits a high-resolution spectrum (not shown), whereas the liquid crystalline phase exhibits a spectrum with very broad lines and low S/N (Figure 4, inset). (iii) In the liquid crystalline phase, the *nonspinning* spectrum is rather featureless as in conventional high-resolution spectra, whereas high-resolution ^{13}C spectra can be obtained for the isotropic phase without MAS spinning (Hamilton et al., 1977; Ginsburg et al., 1982).

The two different kinds of liquid crystalline phases, cholesteric and smectic, were examined in detail by ^{13}C MASNMR. We also compared the metastable liquid crystalline phases of cholesteryl oleate with the stable liquid crystalline phases of cholesteryl myristate. As illustrated in Figure 5, substantial differences between smectic (left panel) and cholesteric phases (right panel) are observed in the region of 45–180 ppm. The smectic phase shows three general

features: (i) the ^{13}C peaks are *narrower* than corresponding peaks for the cholesteric phase; (ii) changing the MAS spinning rate changes the SSB distribution but has little effect on the line shapes and line widths of the central peaks; and (iii) changing the temperature within the same phase does not significantly change peak line shape or line width. In the cholesteric phase, peaks for carbons with a large chemical shift anisotropy (e.g., C=O, C5, C6, C3) are significantly broader than the corresponding peaks in smectic phase. A decrease in the MAS spinning rate causes further line broadening, especially for C=O and C5; the C6 signal is less affected, and the C3, C14,17, and C9 signals are only slightly affected. Peaks in the upfield region (10–40 ppm) are not as obviously affected by varying the spinning rate from 2 to 4 kHz (spectra not shown, see discussion below). An increase in the sample temperature causes line narrowing for the C=O, C5, and C6 peaks but has little effect on the other peaks. Such characteristic line broadening effects provide criteria to distinguish the cholesteric phase from smectic or isotropic phases, and these effects are independent of the stability of the mesophases.

Comparison of spectra of cholesteryl myristate in the smectic phase (Figure 5E) and in the bilayer crystal (Figure 2C) shows that the nonequivalence between the A and B molecules observed in the crystalline phase is lost upon the transition to the smectic phase; i.e., the two peaks observed for several carbons (e.g., C=O, C5, C6, C10, C13, C18, C19, ω-CH_3, etc.) merge into one. The loss of heterogeneity indicates increased molecular motions in the smectic phase which average the different environments that were present in the crystal.

The ^{13}C spectra of the isotropic phase of cholesteryl oleate and myristate have the same general features as erucate (Figure 4C). The values of chemical shift of these two cholesteryl esters in liquid crystalline and isotropic phases are also given in Table II.

^{13}C Spin-Lattice Relaxation Times (T_1) of Cholesteryl Erucate in Different Phases

Comparison of the ^{13}C MASNMR spectra of crystalline cholesteryl esters (Figures 1B, 2A–C, and 4A) shows that the line broadening of the protonated steroid ring carbons compared to the acyl chain and isooctyl side chain carbons is common to all esters. Since such differential line broadening effects (and the dephased CPMAS spectrum, Figure 1B) suggest differing molecular motions, T_1 was measured for cholesteryl erucate in crystalline, smectic, and isotropic states. Table III gives T_1 values of several well-resolved peaks. In the crystalline state, the carbon nuclei can be divided into two extreme groups: one with very long (20–37 s) and the other with short T_1 values (0.8–3 s). Those with long T_1 values are protonated steroid ring carbons and the nonprotonated C=O, C5, C10, and C13 carbons. Carbons with short T_1 values belong to the acyl and isooctyl chains and the angular methyl groups. The rates of molecular motions of these two groups of carbons therefore are quite different. In the smectic phase, the carbon nuclei can be redivided into two new groups: one with moderately long T_1 values (the nonprotonated carbons as well as the terminal methyl group in the ester chain) and the other with rather short T_1 values (the protonated steroid ring carbons). Carbon nuclei belonging to the steroid ring (as well as the C=O) all show a large decrease in T_1 values compared to the crystalline phase. Changing from the smectic to the isotropic phase does not result in large changes in the T_1 values, suggesting similar patterns of high-frequency local motion in the liquid crystalline and isotropic states (Adebodun et al., 1992).

Table III: Values of the ^{13}C T_1 (s) for Cholesteryl Erucate in the Different Phases (Estimated Error about 10%)

peak assignment	MLII	smectic	isotropic
C5	34	1.7	1.3
C=C	1.4	0.59	0.55
C6	37	0.24	0.18
C3	20	0.28	0.16
C14,17	23	0.25	0.23
C9	22	0.35	0.23
C13	22	2.2	1.7
C10	20	*a*	*a*
bCH_2	1.5	0.39	0.29
(ω-2)CH_2; C7,8	*a*	0.55	0.53
$(CH2)_n$	1.8	0.4–0.6	0.45–0.50
C – C=C	1.6	0.53	0.59
	1.1	0.53	0.59
C26,27	2.8	1.1	1.1
(ω-1)CH_2	1.9	1.1	1.1
C21	0.80	0.59	0.54
ω-CH_3	3.0	2.8	3.0
C18	1.2	0.95	0.87

[a] Not clearly resolved.

Attempts to measure T_1 values for crystalline cholesteryl esters with *MLI* (C11:0) and bilayer (C14:0) structures were not successful because the relaxation rates for the "rigid" carbons in these two cases are too slow to be measured within a reasonable time. For the C=O, C5, and C6, there was very little signal intensity decay during relaxation delay times of up to 50 s, indicating the T_1 values are $\gg$50 s. T_1 values of the relatively more mobile carbons, such as the acyl carbons (ω-1)CH_2 and ω-CH_3 and the methyl carbons C18 and C21, are about 2–5 s for *MLI* and bilayer cholesteryl esters (data not shown), slightly longer than T_1's for the *MLII* ester [(C22:1), Table III].

Solid Phases Formed Out of the Liquid Crystalline Phases

Having characterized pure phases of cholesteryl esters by MASNMR, it was of interest to examine mixtures of different phases, since these may occur in biological samples (Small, 1988; Snow & Phillips, 1990; Snow et al., 1992). In these experiments, we observed the formation of a solid phase from undercooled metastable systems and the melting of solid phases in mixed systems.

For cholesteryl esters which form stable mesophases (e.g., cholesteryl erucate and myristate) the smectic–crystalline phase transition is a reversible process, and recrystallization from the smectic phase is completed within hours. The ^{13}C spectrum (not shown) of the crystalline phase thus formed is identical to that obtained before the heating cycles. However, for a cholesteryl ester which forms metastable mesophases (e.g., oleate), solidification can occur at a temperature below the crystal melting temperature, and the recrystallization may not be complete even after a long period of incubation.

Solidification of cholesteryl oleate from a cholesteric or smectic phase is represented in Figure 6. The first three spectra (Figure 6A–C) were taken after different incubation times following cooling from the isotropic phase to 46 °C (1 °C below the isotropic–cholesteric transition temperature). A CPMAS spectrum taken after 2.5 h (Figure 6A) shows that the major part of the sample has become solidified, since CP significantly enhances the ^{13}C signal, and two distinct sets of peaks are seen for the C=O, C5 and C6. Among these two sets of peaks, one has the same chemical shift values as those for the *MLII* crystalline phase, while the other set is closer to the chemical shift values in the noncrystalline phase (Table I). Multiple peaks for the same carbon are also observed in the region of 10–45 ppm; notably, the ω-CH_3 appears as three

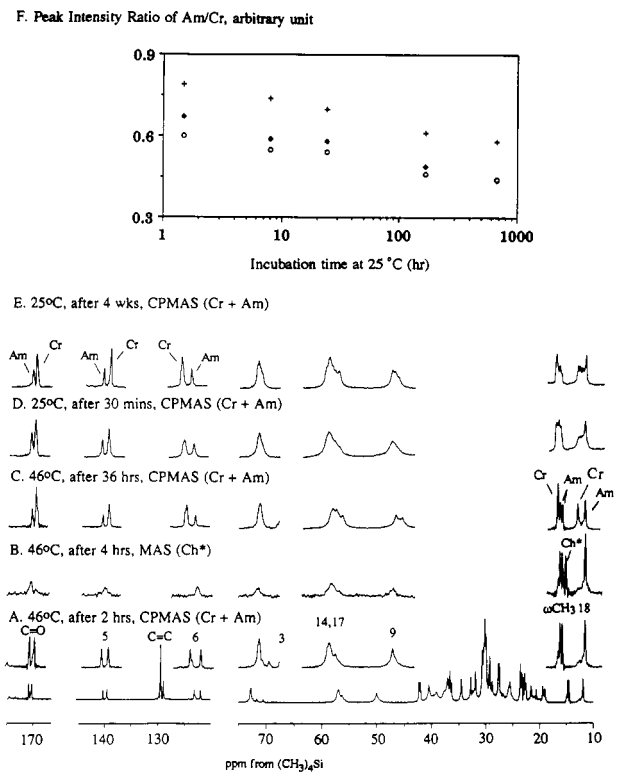

FIGURE 6: ^{13}C MASNMR spectra of cholesteryl oleate cooled from the isotropic liquid phase. All spectra were otained with 2400 scans and a spinning rate of 4.0 kHz; selected regions are shown with vertical and horizontal expansions. (A) CP spectrum taken after 2 h of incubation at 46 °C, showing a mixture of the *MLII* crystals (Cr) and a solid state amoprhous phase (Am); (B) spectrum without CP, taken after 4 h of incubation at 46 °C, showing mainly the cholesteric phase (Ch*); (C) CP spectrum taken after 36 h of incubation at 46 °C, showing a mixture of Cr and Am; the peak intensity ratio of Am/Cr is reduced compared to spectrum B, showing the rearrangement of the Am phase to the Cr structure; (D) CP spectrum taken after 30 min of incubation at 25 °C, showing a mixture Cr and Am; (E) CP spectrum taken after 4 weeks of incubation at 25 °C, showing a mixture Cr and Am; the reduction of the peak intensity ratio of Am/Cr indicates the rearrangement of the Am phase to the Cr structure; (F) the peak intensity ratio of Am/Cr as a function of incubation time at 25 °C for C=O (◆), C5 (○), C6 (+).

well-resolved peaks (Figure 6A). The most downfield peak corresponds to the crystal structure, and the two upfield peaks likely arise from the second solid phase. There are also multiple signals for C18.

Figure 6B shows selected regions of a spectrum taken immediately after that of Figure 6A with the same conditions except without CP. The appropriate pulse repetition rate is no longer determined by the ^1H $T_{1\rho}$ (T_1 of ^1H in the rotating frame) values but by the much longer ^{13}C (T_1 values, and the resonances with long T_1 values will be saturated by the short pulse interval used. Thus, the spectrum (Figure 6B) does not show signals for rigid carbons in the solid state (e.g., C=O, C5, C6, C3) but shows weak and broad peaks similar to those of the cholesteric phase (Figure 5F). In the region of 10–20 ppm (Figure 6B), there are four well-resolved peaks for the ω-CH_3; among these, the most upfield one (14.1 ppm) was not observed with CP (Figure 6A) and reflects ω-CH_3 with fast thermal motions. Therefore, Figure 6 panels A and B together show that the sample is a mixture of three coexisting phases: *MLII* crystals, amorphous solid, and the cholesteric liquid crystal.[2] Extension of the incubation time at the same temperature (46 °C) causes little change in the cholesteric phase (spectrum not shown). A spectrum taken with CP after 36 h (Figure 6C) shows a significant increase in the relative intensity of peaks for the crystalline cholesteryl ester compared to the second solid phase (compare with Figure 6A). However, such conversion is still far from completion, implying the rearrangement is very slow.

When cholesteryl oleate is cooled from the isotropic to the smectic phase and then to 25 °C, the solid state thus formed is also a mixture of *MLII* crystalline and the second solid phase. However, at this temperature a liquid crystalline phase is not detected either by ^{13}C or ^1H NMR (spectra not shown). The CPMAS spectra (selected regions) taken after incubation of cholesteryl oleate at 25 °C for 30 min and 4 weeks (Figure 6D,E) reveal a very slow rearrangement of the second solid phase into the *MLII* crystalline phase. Figure 6F gives the intensity ratio of the second solid phase peak to the crystalline peak for C=O, C5, and C6 as a function of incubation time and shows that the half-life time of the second solid phase is more than 1000 h.

Additional experiments were conducted to characterize this phase. First, the chemical shift anisotropy values measured from the two sets of C=O peaks in the solid mixture are very close to each other,[3] additional evidence that the second set of the ^{13}C signals represents another solid phase. Second, X-ray powder diffraction patterns were obtained for cholesteryl oleate samples which consisted of pure *MLII* or a mixture of *MLII* and the second solid phase. The lamellar long spacing (d) values calculated from the diffraction pattern in both samples are identical (data not shown) and agree with the d values of single crystalline cholesteryl oleate in the literature (Craven, 1979). The second solid phase is therefore probably not a crystalline structure[4] but, more likely, an amorphous phase, consistent with the observation that the ^{13}C signals do not correspond to the other crystal structures investigated (Table I).

Figure 7 shows ^{13}C MASNMR spectra of the cholesteryl oleate solid state mixture (*MLII* crystals and amorphous) at various temperatures in the reheating process (from 25 to 51 °C) to the isotropic phase. At 47 °C (Figure 7A) the major component in the CPMAS spectrum reflects the *MLII* crystalline form (as in Figure 6A), but a significant amount of amorphous solid is observed. The intensities of the signals corresponding to the amorphous phase decrease as the temperature increases. At 48 °C (Figure 7B) the CPMAS spectrum is essentially that of *MLII* crystals, with a trace amount of amorphous solid left. For comparison, a spectrum (Figure 7C) was obtained as above (Figure 7B) except that without CP, so that steroid ring peaks originating from the solid state (e.g., C5, C6, C10, C13) are significantly suppressed. The observed signals for these carbons (Figure 7C) originate mainly from the coexisting cholesteric phase (compare also with Figure 6B). Since signals for the isotropic phase are not detected at 48 °C (Figure 7C), it is likely that the amorphous solid melts into the cholesteric phase rather than into the

[2] With CPMAS, it is difficult to quantitate the liquid crystalline and solid phases accurately because the CP enhancement for the solid phases differs from that for liquid crystalline phase. It is possible to use MASNMR without CP contact and with a very long preacquisition delay (about 100 s) to quantitate signals in the solid state and a shorter delay (about 5 s) to quantitate the signals in the liquid crystal state, but the time required for such an experiment is very long.

[3] Unpublished data in this laboratory.

[4] It is possible, but unlikely, that a different crystalline form could produce differences in the environment of the steroid ring as seen by NMR but no difference in the X-ray powder diffraction pattern.

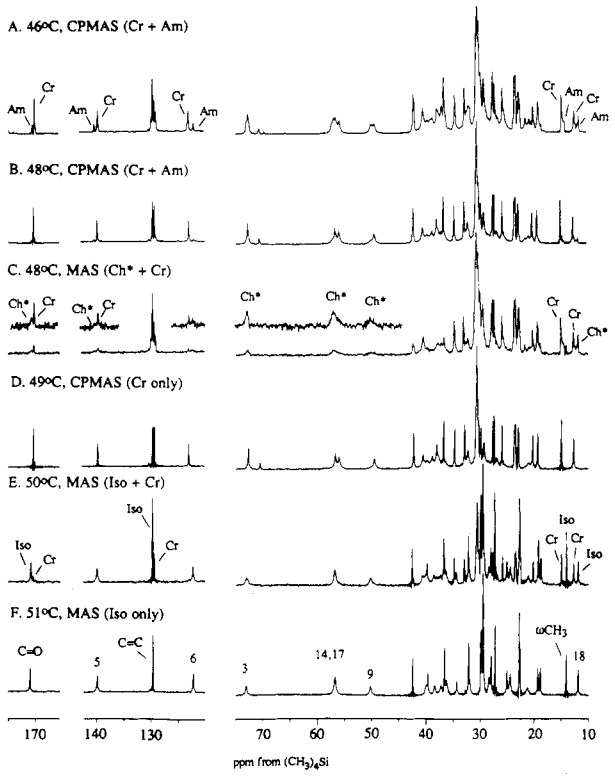

FIGURE 7: ^{13}C MASNMR spectra of cholesteryl oleate reheated from a mixture of solid phases (see Figure 6) at 25 °C, with a spinning rate of 4.0 kHz and 2000 scans, excepted as noted: (A) CP spectrum at 46 °C, showing a mixture of Cr and Am, (B) CP spectrum at 48 °C, showing mainly Cr and a trace amount of Am; (C) spectrum at 48 °C without CP, showing mixture of Cr and CH*; (D) CP spectrum at 49 °C, shows only Cr; (E) spectrum at 50 °C without CP, showing a mixture of Cr and the isotropic liquid phase (Iso); (F) spectrum at 51 °C without CP, showing only Iso (640 scans).

isotropic phase. At 49–50 °C only one set of ^{13}C peaks, corresponding to *MLII* crystals, is observed with CPMAS (e.g. 49 °C, Figure 7D). The two peaks for the 9 and 10 carbons of the olefinic (~130 ppm) are of equal intensity, implying that the amorphous phase is mostly melted. The isotropic phase starts to become observable at 49 °C in the spectrum without CP (spectrum not shown) and coexists with *MLII* crystals at 50 °C (Figure 7E). Since Figure 7E is obtained without CP, crystalline peaks for the rigid carbon nuclei (e.g., C5, C6) are not observed, but carbons such as the oleate C=C, the angular methyl C18, and ω-CH_3 are flexible enough to give significant signals, indicative of the *MLII* crystalline phase. At 51 °C the CPMAS spectrum collapses into complete noise (not shown), annd the spectrum obtained without CP reflects a pure isotropic phase (Figure 7F).

DISCUSSION

An important reason for the use of solid state NMR spectroscopy is to make correlations between the structure of a sample and the chemically inequivalent resonances representing this structure (Bovey, 1988). This goal can often be achieved with magic angle spinning and high-power decoupling, which reduces the very broad lines of a solid or liquid crystalline sample to narrow lines at the isotropic chemical shift. The success of this approach is illustrated in the present studies of solid and liquid crystalline cholesteryl esters. The very high resolution obtained in ^{13}C spectra of crystalline and liquid crystalline cholesteryl esters permits elucidation of structural and dynamic features at numerous atomic sites within the molecule.

^{13}C Chemical Shift and Structural Heterogeneity in Crystalline Cholesteryl Esters. In this work cholesteryl esters of three typical crystalline structures have been examined by CPMAS NMR. The ^{13}C chemical shifts are interpreted in terms of the known crystal structures. For cholesteryl esters with *MLII* structures (C18:1, C22:1, and C6:0), the unit cell is composed of two symmetrically related, antiparallel molecules (Figure 8A; Craven, 1986). In the center of the monolayer, there is an efficient packing of cholesteryl ring systems to form stacks of molecules. Ring–ring interactions are dominant in this type of crystal structure, and ring–chain or chain–chain interactions are less important. Since all the molecules in the crystal are essentially equivalent, only one peak for each carbon is expected. As shown in Figure 1 and Table I, cholesteryl esters with *MLII* structures give only one chemical shift value for each carbon nucleus. The chemical shifts of corresponding nuclei are generally quite similar for the three esters investigated, indicating little influence of the acyl chain on the environment of the steroid ring in the crystal. In addition, the chemical shift values for the *MLII* crystals are generally close to those in the liquid crystalline and isotropic states (Tables I and II). Differences range from 0 to 1.5 ppm; the largest differences are seen for carbons that are expected to gain mobility, and possibly experience changes in local environment, when the crystalline state melts into a noncrystalline state (e.g., C18, C19, C21, C26, C27, and the ω-CH_3). Several steroid ring resonances (e.g., C5, C6, C3) for *MLII* crystals have chemical shifts that are significantly different from those of the two other crystal forms (Table I). Interestingly, these differences vanish in liquid crystalline and isotropic states, and the chemical shift values in noncrystalline states lie closer to those for the *MLII* esters than for the *MLI* or bilayer esters (Table II).

Cholesteryl esters with *MLI* structures (cholesteryl decanoate and undecanoate; C10:0 and C11:0) contain two types of molecules (A and B) that are unrelated by crystal symmetry (Figure 8B; Craven, 1986). One of these molecules (B) exists in antiparallel stackings, similar to those in *MLII*. Molecules A have a different arrangement, with the steroid rings almost perpendicular to those of molecules B. There is a gradual transition between regions of close packing within the monolayers and loose packing in the interface region between monolayers. The change in the ester chain length has little effect on the molecular arrangements in the central region but does cause some difference in the packing in the interlayer region, which affects the thickness of the monolayers (Craven, 1986).

Because of the restricted internal mobility of the molecules in the crystalline state, nuclei at different conformational sites but identical in other respects can give different signals (Moller et al., 1984). The inequivalence of several carbon signals in the spectra of *MLI* can be explained by the nonequivalent chemical environments of molecules A and B. By examining the crystal structure of *MLI* (Figure 8B), it is seen that the two A molecules are arranged in such a way that the two carbonyl groups are located next to each other, whereas the two carbonyl groups of the B molecules are separated by a distance of the cholesteryl rings. Such an arrangement permits stronger intermolecular interactions between the two carbonyl groups in A molecules and makes the chemical shielding on the C=O (A) much larger than that on the C=O (B). The upfield (more shielded) signal is therefore assigned to C=O (A). The assignments (Table I) of A and B molecules for other nonequivalent ^{13}C signals, such as C3, C5, C6, and C9, are based on similar considerations of shielding effects caused by the different conformational sites. These assignments are independent of the ester chain lengths.

A. Monolayer II (*MLII*, C18:1, C22:1, C6:0)

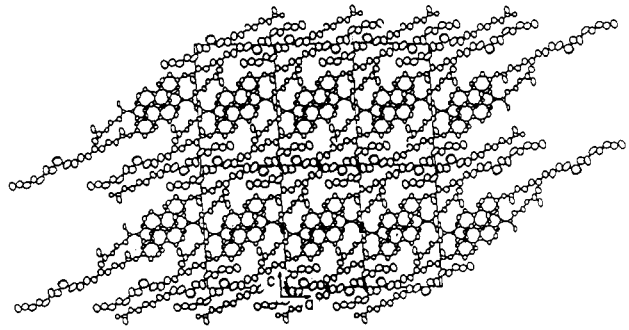

B. Monolayer I (*MLI*, C10:0, C11:0)

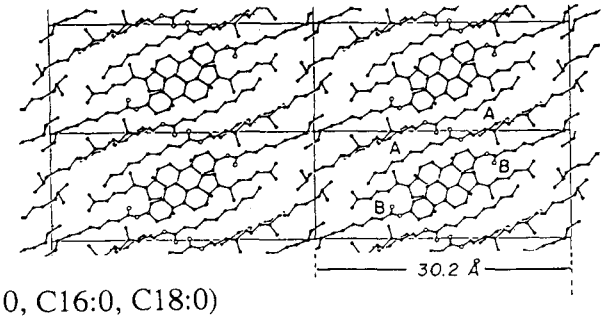

C. Bilayer (C14:0, C16:0, C18:0)

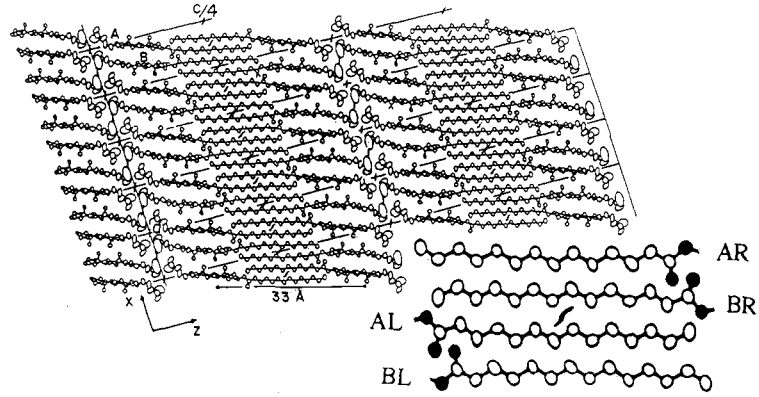

FIGURE 8: Crystalline packing structures for cholesteryl esters, according to Craven (1986): (A) monolayer II (*MLII*); (B) monolayer I (*MLI*); (C) bilayer. The inset represents the enlarged portion of the bilayer stratas.

Nonequivalence of carbons is also seen for methyl resonances of *MLI* crystals. In the 10–18 ppm region (Figure 2A,B) there are three peaks, which belong to the ω-CH_3 of the ester chain and the steroid C18. For cholesteryl decanoate, only one peak was found for the ω-CH_3, but a pair of slightly separated peaks was seen for the C18. For cholesteryl undecanoate, one peak was found for C18, but two well-separated peaks were found for the ω-CH_3 (15.78 and 14.25 ppm). Because the A chain is packed between two steroid rings and is expected to be less mobile than B chain (Craven, 1986), the broader downfield signal is assigned to the A molecule. We speculate that only one peak is observed for the ω-CH_3 of C10:0 because the acyl chains are twisted for a closer monolayer packing (Craven, 1986), and such an arrangement happens to cancel the difference of the CH_3 groups between A chain and B chain. This might also explain the small separation between the two C18 signals of C10:0, because C18 (A) is next to the middle section of the B acyl chain and C18 (B) is next to the middle section of the A acyl chain; i.e., both are in similar environments. The twisting of chains would have to change the environment slightly around C18 to produce two different environments; however, at this point there is not enough information to determine which one is more shielded. In crystalline C11:0, both acyl chains are fully extended (Craven, 1986), and the shielding on C18 from A and B is the same, so that only one peak is observed. Complete assignments for esters with the *MLI* structure are summarized in Table I.

The bilayer crystal structure is common to cholesteryl esters with long saturated chains, such as C14:0, C16:0, and C18:0, and exhibits efficient chain packing within the bilayers, which is lacking in the monolayer structures. An increase in the length of the acyl chain causes an increase in the bilayer thickness but has little effect on the packing of the cholesteryl ring systems. Comparison of the steroid ring resonances reveals almost no variations in chemical shift with chain length (Table I), whereas resonances of *MLI* crystals show small variations even for the closely related chain lengths (C10:0, C11:0). Cholesteryl esters with a bilayer structure are also composed of two inequivalent molecules A and B, but the molecular arrangement is different from that in *MLI* structure (Figure 8C, Craven, 1986). In this case the difference in the conformations between A and B molecules is clearly seen only for carbons in the cholesteryl core structures.

Assignments of inequivalent resonances can be made (as for the *MLI* crystal) on the basis of shielding effects caused by the immediate environment. The angular methyl groups are interesting examples because the chemical shift difference for A and B molecules is very large for C18 (1.75 ppm) compared to C19 (0.41 ppm). In the molecular arrangement (Figure 8C), the C18 and C19 methyls project between neighboring molecules. C18 (A) is locked between the C19 (B) and C18 (B), whereas C18 (B) is surrounded by C18(A) and the flexible isooctyl group, so that C18 (A) is more shielded than C18 (B). Similarly, C19 (B) is locked between C18 (A) and C19 (A), and is thus more shielded, but C19 (A) is surrounded by C19 (B) and the interdigitated acyl chains, which are less mobile than the isooctyl group. Therefore, the shielding difference between C19 (A) and C19 (B) is much smaller than that between C18 (B) and C18 (A), as reflected in their chemical shift values (Table I). Shielding differences were also considered in making assignments to other resonances which showed two signals (C5, C6, C10, C13, Table I).[5]

In the bilayer structure the acyl chains are located in the inner stratas with restricted close packing, a different arrangement from the monolayer crystals (Craven, 1986). As shown in Figure 8C, if the molecules with cholesteryl rings on the left and the right sides of the inner stratus are denoted as "L" and "R", respectively, symmetry requires that the immediate environments of nuclei in AL and BR are equivalent (and AR = BL). This implys that, for the carbons in the *acyl chains*, the nonequivalence between molecules A and B is no longer simply described by A $\neq$ B; instead, it is characterized by AR = BL $\neq$ AL = BR (Figure 8C, inset). For example, all the carbonyl groups are arranged such that the carbon nucleus has about the same distance to the double bond oxygen in the neighboring molecule, but the carbonyl in AL is also close to the bridge oxygen in BL, whereas that in BL is farther away from the bridge oxygen in AL. On the other side, the carbonyl carbon in AR is farther away from the bridge oxygen in BR, but that in BR is close to the bridge oxygen in AR (the actual distances C···O in either case are the same as that on the left side). Therefore, C=O (AL and BR) experiences a greater shielding than C=O (AR and BL). Similarly, the ω-CH_3 in the acyl chains of AL and BR molecules is more shielded than the ω-CH_3 of AR and BL. The shielding difference on the (ω-1)CH_2, which produces two signals for this carbon, is likely to be due mainly to the induction effect of the ω-CH_3. The assignments of peaks based on the discussion above are presented in Table I.

Molecular Motions of Crystalline and Liquid Crystalline Cholesteryl Esters. In the ^{13}C MASNMR spectrum of crystalline cholesteryl esters (Figure 1B,2, and 4), the peaks from the protonated steroid carbons are generally broader than the acyl chain carbons or the nonprotonated steroid carbons. On a theoretical basis, such line broadening could be caused by (1) interference effects between the C–H dipolar coupling and the ^{13}C chemical shift shielding tensors (Oldfield et al., 1991); (2) the incoherent spatial modulation caused by motions which interfere with the coherent modulation of the rf decoupling (Rothwell & Waugh, 1981); or (3) motional modulation of the chemical shielding interaction, which can be particularly important for nonprotonated carbons having large chemical shielding anisotropies (Suwelak et al., 1980; VanderHart et al., 1981). In the present case, mechanism 1 can be excluded since high-power dipolar decoupling is applied in our experiments. Mechanism 3 can also be excluded since there is no line broadening effect observed for the C=O and C5 carbons, which possess the largest chemical shift anisotropies. Therefore, the line broadening for the protonated steroid carbons is most likely due to the fact that the thermal motion of these nuclei are on a time scale that interferes with the ^1H–^{13}C dipolar coupling field and results in the insufficient decoupling effect (Smith et al., 1987). The motions of the terminal portion of the acyl chain, the isooctyl methyls, and the angular methyls are relatively fast compared to the steroid ring and do not fall into the above category, as shown by the dephased CPMAS experiment in Figure 1B. These carbons with faster molecular motions are the same carbons that show poor resolution in the crystal structure of cholesteryl esters at 25 °C (Craven, 1986).

^{13}C spin–lattice relaxation time (T_1) measurements for crystalline (*MLII*) cholesteryl erucate (Table III) reveal that carbons with relatively broad peaks (C6, C3, C14,17, C9) have very long T_1 values. The nonprotonated carbons which are part of the steroid ring (C5, C10, C13) or closely attached to it (C=O) have similarly long T_1 values even though the lines are narrow. The general requirement for T_1 relaxation is a magnetic interaction fluctuating at the resonance frequency. The major physical mechanisms that provide such relaxation conditions are (1) dipolar interactions, modulated by molecular tumbling (both intermolecular and intramolecular interactions) or by translational diffusion (intermolecular interactions); and (2) shielding anistropy (the shielding on a nucleus, and therefore the magnetic field acting on it), which varies with the molecular orientation in the static field B_o. Molecular tumbling therefore modulates the local magnetic field and causes relaxation. Although we can not distinguish which mechanism makes a larger contribution, the same type of molecular motions are important in both. Therefore, the very long T_1 values for the steroid carbons are due to the very slow molecular motions of the steroid rings in the *MLII* structure,[6] which result in weak fluctuating fields and very slow relaxation. The T_1 values of steroid carbons in cholesteryl esters with *MLI* or Bilayer structures were significantly longer ($T_1 > 50$ s) than those of the *MLII* crystals. In these two crystalline structures, the closer packing of the steroid rings evidently further slows down their molecular motions and reduces the spin–lattice relaxation rates compared to the *MLII* crystals.

The acyl chains in the *MLII* crystal are located mainly in the interface region between monolayers with no repeating subcell pattern (Figure 8A) (Craven, 1986). These chains are loosely packed with considerable disorder and thermal motion; thus, they are much more mobile and undergo rather fast relaxation. In the crystal structures (Figure 8), the acyl chains in cholesteryl esters become more organized in the order of *MLII* < *MLI* < bilayer, but the T_1 values of the terminal groups [e.g., (ω-1)CH_2 ω-CH_3] increase only slightly

[5] Since C10 and C13 are well isolated from intermolecular contact, the chemical shift differences between A and B for these two nuclei directly originate from the induction effects of C19 and C18. For C5 and C6, the major difference between the intramolecular shielding should be from the through-bond induction effect from C19 to C10 and then to C5 and C6. However, this can not explain why the separation between the two signals for C10 and C19 is about 0.2–0.3 ppm, whereas that for C5 and C6 is 0.4–0.6 ppm. Careful examination of Figure 8C again shows that the C5 and C6 in A are rather close to C19(B), whereas C5 and C6 in B molecule are close to C18(A). Since C18(A) is much more shielded than C19(B), the through-space interaction may cause the shielding on C5 and C6 (B) to be slightly larger than that on C5 and C6 (A). Therefore, the shielding difference caused by the intramolecular induction effect might be amplified by the through-space dipolar interaction between the double bonds, i.e., the C5 and C6 in B molecule is more shielded than those in A molecules.

[6] Solids with slow motions will lie on the right-hand branch of the T_1 curve for isotropic rotation, where longer T_1's reflect slower motions (Bovey, 1988).

in this order. Because of inadequate resolution, T_1 values for carbons in the middle or near the beginning of the acyl chain could not be determined accurately for esters without unsaturation in the acyl chain (*MLI* and bilayer esters).

When the crystalline phase melts into a liquid crystalline phase, the slow and restricted motions of the steroid rings are replaced by fast tumbling and lateral diffusion within the layers, which results in a drastic reduction of T_1 values for the ring carbons (Table III). A slight narrowing of some steroid ring ^{13}C resonances accompanies this transition. The transition from a liquid crystalline phase to the isotropic phase is accompanied by much less effect on the corresponding T_1 values. This is probably because the high-frequency local motions in liquid crystalline and isotropic states are not much different from each other (Adebodun et al., 1992). Similarly, because the acyl chains are undergoing fairly rapid motions even in the crystalline phase, the change in T_1 values for the acyl chain carbons is small compared to that of the ring carbons on going from the crystalline to liquid crystalline and then to the isotropic state.

Phase Transitions Observed by ^1H NMR. Unlike the ^{13}C MASNMR spectra, the ^1H MASNMR spectra of crystalline cholesteryl esters are very broad and featureless (Figure 3D). This is because the static dipolar Hamiltonian does not commute with itself for proton pairs with different orientations (Forbes et al., 1988), and the MAS spinning rate is not enough to overcome such strong *homonuclear* coupling interactions. In liquid crystalline phases, the intermolecular dipole–dipole interactions are averaged by fast lateral diffusion. MAS also partially reduces the *intramolecular* dipole–dipole interaction, causing the angular dependence of the Hamiltonian to be the same for all proton pairs. Therefore, even with the MAS spinning rate much slower than the static spectra breadth, the static line shape is broken down into numerous sharp spinning side bands (Forbes et al., 1988a,b). Since such a change in the ^1H spectrum is very sensitive and reproducible, the appearance of the SSB can be used as an indication of the solid–smectic phase transition for cholesteryl esters (Figure 3C,D). As the temperature is increased in smectic phase, the SSB intensity increases gradually with the basic pattern unchanged.

At the transition from the smectic to the cholesteric phase, there is an abrupt decrease in the intensity of SSB's (Figure 3B,C), and the overall static line width (Forbes et al., 1988a) is also significantly reduced. These changes are due to a decrease in the overall dipolar interaction caused by increased disorder and increased rates of molecular motions in the cholesteric phase, which not only average out intermolecular but also partially average out intramolecular, dipole–dipole interactions (Forbes et al., 1988a,b). At the same time, the smectic to cholesteric phase transition is also accompanied by the significant line broadening of both the central peak and the SSB's (Figure 3B,C), which is most likely caused by the fact that in this phase, the average residual dipole–dipole interaction is comparable to the MAS spinning rate, so that MAS spinning no longer reduces the line width effectively. Another possible reason for such line broadening is the larger distribution of the isotropic chemical shift (see below). Such a pattern remains until the transition from cholesteric phase to isotropic phase, at which point the center peak becomes very sharp again and the side band intensity is reduced to a negligible level (Figure 3A). The spectrum contains high-resolution features, as previously described (Kroon, 1981). It should be emphasized that although the ^1H spectra do not provide as much quantitative information about molecular structure and motions of cholesteryl esters in crystalline and liquid crystalline phases, they provide a clear method of distinguishing each different phases.

^{13}C MASNMR of Liquid Crystalline and Isotropic Phases. High-resolution ^{13}C NMR spectroscopy has previously been used to characterize the isotropic and liquid crystalline phases of cholesteryl esters, particularly the isotropic phase, which gives a highly resolved spectrum (Hamilton et al., 1977; Ginsburg et al., 1982; Croll et al., 1985; Croll et al., 1986). Liquid crystalline phases give characteristic spectra, in which the signals for steroid ring carbons and carbons in the acyl chain close to the ester linkage are broadened beyond detection, whereas signals for several acyl chain carbons are narrow enough to be detected. These changes on going from the isotropic phase to liquid crystalline phases reflect the marked decrease in molecular motions accompanying the phase change. These spectra reveal the relative fluidity of the ends of the acyl chains in liquid crystals. The differences between spectra of cholesteric and smectic liquid crystalline phases are subtle: the resonances seen in the cholesteric phase broaden slightly in the smectic phase (Hamilton et al., 1977). A further broadening of the few carbon resonances seen for liquid crystalline cholesteryl ester occurs in the crystalline phase, and no signals are detected for solid cholesteryl ester under typical "high-resolution" experiment conditions (Hamilton et al., 1977; Croll et al., 1985).

In contrast, ^{13}C MASNMR spectra of the different phases of cholesteryl esters differ less markedly (Figure 4). All phases show resonances for carbons throughout the molecule and exhibit similar differential line broadening (i.e., broader resonances for protonated steroid ring carbons). On going from the crystalline to the smectic phase, a slight narrowing of steroid ring resonances, particularly those of protonated steroid carbons (Figure 4A,B), is seen. In addition, for cholesteryl esters with the *MLI* or bilayer structure, the inequivalent peaks of the same carbon all merge into one (Figure 5D,E) upon loss of the nonequivalent chemical environments of individual molecules. The ^{13}C MASNMR spectrum of the smectic phase (Figure 4B) bears a close resemblance to that of the isotropic phase (Figure 4C), except for the presence of some weak SSB's in the spectrum of smectic phases.

The cholesteryl esters studied can exist in three different crystalline structures but have two different smectic phases. Cholesteryl esters with saturated acyl chains usually exist in a smectic A structure, and those with unsaturated acyl chains in a smectic C structure. In both cases the molecules are arranged in a layered structure, but in smectic A the layer normal is parallel to the director (long molecular axis) and in smectic C the director is tilted to the layer normal by a certain angle. Although smectic A and smectic C differ in many physical properties (optical, dielectric, etc.), the molecular packing and motions in both phases are similar (except for the angle between the director of smectic C and the layer normal). This can be further illustrated by the close resemblance of the chemical shift values for different cholesteryl esters in smectic phases.

A comparison of chemical shifts of crystalline cholesteryl esters (Table I) shows that cholesteryl myristate (bilayer) exhibits rather different ^{13}C chemical shifts compared with cholesteryl oleate and erucate (both *MLII*). However, in the smectic phase cholesteryl myristate (smectic A) and cholesteryl oleate or erucate (smectic C) give about the same the chemical shift values (Table II), which are close to those of the *crystalline* cholesteryl oleate or erucate (*MLII*). This implies a common molecular organization of the smectic phase for different esters; furthermore, the organization is closer to that in the *MLII* crystals than in the bilayer crystal. Therefore, for cholesteryl

myristate the bilayer structure must change into a monolayer structure to form the smectic phase, while, for cholesteryl erucate, the *MLII* to smectic phase transition involves a less drastic molecular rearrangement. Such differences could account for the fact that the enthalpy and entropy changes for the crystalline to smectic phase transition for cholesteryl myristate [ΔH = 11.40 kcal/mol; ΔS = 33.2 cal/(mol·deg) (Barrall & Johnson, 1974)] are more than twice as much as those for cholesteryl erucate [ΔH = 5.16 kcal/mol; ΔS = 16.2 cal/(mol·deg) (Ginsburg & Small, 1981)]. In support of this interpretation, electron diffraction (Dorset, 1985) detected a pretransition crystal form near the crystalline to smectic phase transition of cholesteryl myristate which might account for the molecular reorientation from a bilayer crystalline structure to a monolayer-like smectic structure.

On going from the smectic to the cholesteric phase, ^{13}C MASNMR spectra show a characteristic line broadening for several carbon peaks, especially the C=O, C5, and C6 (Figure 5), whereas other peaks in the spectrum are essentially unaffected. Because the current spectra are obtained with proton decoupling, and the lines with most broadening (C=O, C5) are from nonprotonated carbons, such line broadening is not likely to be due to insufficient decoupling. Instead, the differential line broadening in the cholesteric phase is most likely to be due to a distribution of chemical shifts caused by the motional modulations of the chemical shielding.

To understand why such a significant distribution of ^{13}C chemical shift exists in the cholesteric phase but not in the smectic phase, the difference in molecular arrangement and molecular motion in these two types of liquid crystalline phases must be considered. The smectic phase is characterized by layers that are flexible to glide over each other, via free lateral diffusion of individual molecules within each layer, and by intralayer molecular spacings that lack the uniformity of a true crystal (Ginsburg et al., 1984). In general, the chemical environment around individual molecules within such a structure are equivalent. Therefore, the "natural line width" is rather narrow, and with CPMAS a sharp center peak is observed for all the carbons. Molecules in the cholesteric phase are arranged in twisted layers under the influence of chiral centers, which gives rise to a director field of the helical structure (Lafontaine et al., 1989). In addition, there also exist extensive textural defects in most cholesteric liquid crystalline phase (Lafontaine et al., 1989). Therefore, within the cholesteric phase the molecules are not homogeneously aligned along the director as in the smectic phase (Luz et al., 1981). Such structure inhomogeneity thus causes a larger distribution of the isotropic chemical shifts for the carbons in the rigid segments of the molecules, i.e., the steroid rings. Carbons in both the acyl and isooctyl chains are not affected because of the high flexibility of these chains, which makes them insensitive to the orientational ordering of the cholesteryl core. Since the aliphatic region of the ^{13}C chemical shift (10–45 ppm) is dominated by the narrow lines originating from the chain carbons, the line broadening of the ring carbons because of the structure inhomogeneity in the cholesteric phase is not clearly observable. On the other hand, in the downfield region, such line broadening is very significant for C=O, C5, and C6 peaks, among which the C5 peak is the most prominent, because C5 is located at the most rigid part of the cholesteryl core, whereas C=O is partially affected by the acyl chain motion, and C6 by the C–H stretching motion. Since the increase of MAS rate averages part of the bulk phase inhomogeneity, and the increase of temperature reduces the viscosity (and thus the structure defects), they both cause some line narrowing for these carbons in the cholesteric phase (Figure 5F–J). However, the lines in the cholesteric phase are still much broader than those in the smectic phase (Figure 5A–F) because of the differences in their structures.

Although compared to ^{1}H MASNMR, the ^{13}C MASNMR spectra for a given cholesteryl ester in different phases are not as markedly different, the specific phase can be identified by characteristic chemical shifts and line widths of certain resonances and by performing additional NMR experiments. To distinguish a crystalline phase from a liquid crystalline phase for a given cholesteryl ester sample, an effective approach is to perform the ^{13}C MASNMR experiments with and without CP (keeping other experimental conditions constant). A crystalline sample will give a drastic signal enhancement in the CPMAS spectrum, whereas a liquid crystalline sample will give comparable signal intensities in both spectra. T_1 measurements reveal marked changes in steroid ring T_1 values on going from crystalline to liquid crystalline phase (Table III). Smectic and cholesteric phases are distinguished, as described above, by the line widths of unsaturated steroid ring carbons and their response to temperature and spinning rate. In addition, the smectic, but not the cholesteric, phase usually gives some SSB's (which can be readily identified by varying the spinning rate). In the isotropic phase both chemical shift anisotropy and dipolar interactions are averaged to be zero, so that a high-resolution spectra can be obtained with low power ^{1}H decoupling and without magic angle spinning (Hamilton et al., 1977; Ginsburg et al., 1982; Croll et al., 1985). ^{13}C MASNMR thus provides no additional information about the isotropic phase compared to that obtained by high-resolution spectroscopy.

Solid Phases Formed from the Liquid Crystalline Phase. When cholesteryl esters did not consistent of a pure phase, ^{13}C MASNMR spectroscopy proved useful in distinguishing the different phases and monitoring the crystallization processes. The solid state of a few typical cholesteryl esters formed by cooling the liquid crystalline phase was compared with the corresponding stable crystalline phase before the heating process. For cholesteryl esters with stable mesophases (e.g., myristate and erucate), recrystallization occurs rapidly at or below the crystal to liquid crystal phase transition temperature (within 3 h in our experiments), and the ^{13}C CPMAS spectrum of the newly formed solid state is identical to that before the heating process. For example, for cholesteryl myristate the single peaks for C=O, C5, C6, C10, C13, C18, and the ω-CH_3 observed in the smectic phase split into the two sets of peaks observed before heating (Table I), indicating the same bilayer structure.

For cholesteryl esters with metastable mesophases such as cholesteryl oleate, solidification can occur at any temperature below the crystal to isotropic phase transition temperature (Ginsburg et al., 1984). When a solid sample which has been stored at low temperature for a long period and has not been melted is initially examined by ^{13}C MASNMR spectroscopy, one set of peaks for the *MLII* crystal is observed. After melting to the isotropic liquid, followed by incubation in the temperature range of the cholesteric or smectic phase, there are two distinguishable peaks for a number of carbon nuclei in the CPMAS spectrum (Figure 6). The ^{13}C chemical shifts for one set of peaks corresponds to those of the *MLII* crystal (Table I). Although the other peaks are shifted toward peaks of noncrystalline phases (liquid crystalline or isotropic phases), this phase was identified as a solid state(s) by ^{13}C MASNMR experiments. The relative intensities, but not the chemical shift values, of these two sets of peaks are dependent on the incubation temperature and time. The X-ray powder diffraction pattern of cholesteryl oleate before and after the

heating process is identical, showing that one of these two phases is *MLII*. The second solid phase not detected by X-ray is likely an amorphous solid. Conversion of the amorphous phase of cholesteryl oleate into *MLII* is observed during prolonged incubation, but the overall conversion rate is very slow (Figures 6 and 7). A mixture of different crystalline forms has been detected by ^{13}C MASNMR in a related compound, cholesteryl acetate (Webb & Zilm, 1989).

When such a solid state mixture is subjected to reheating cycle, the *MLII* crystals melt to the isotropic phase at the expected melting point (50–51 °C), but the amorphous phase melts 2–3 °C below this temperature (Figure 7). Since the amorphous solid is more disordered, as indicated by its chemical shift values, it is likely that this phase first converts into the cholesteric phase (Figure 7C) before it further melts into the isotropic phase.

^{13}C MASNMR spectroscopy also can be used to distinguish different phases in mixed phase samples. For example, in a mixture of solid and cholesteric cholesteryl oleate, both phases could be observed under conditions of CP (Figure 6A and 7A), whereas the solid phase could be eliminated and the cholesteric phase observed, by eliminating CP and using a shorter recycle time between pulses (Figure 6B and 7C). This represents an important advantage of ^{13}C MASNMR over conventional high-resolution ^{13}C NMR spectroscopy, which cannot distinguish or quantitate different phases in the same sample (Hamilton et al., 1977; Croll et al., 1985). Biological tissues often contain mixed phases because of variations in chemical composition and in droplet size (Small, 1988; Snow et al., 1990, 1992). ^{13}C MASNMR spectroscopy should be extremely useful in characterizing all phases in such complex biological systems.

Conclusion. This work presents a systematic MASNMR study on cholesteryl esters in various physical states. It describes (i) ^{13}C and ^{1}H spectral features that can be used to identify the physical states of cholesteryl ester; (ii) experimental protocols to identify specific phases in mixed phase samples; (iii) ^{13}C spectral features that can be used to identify the specific crystalline structure and illuminate details of the crystal molecular organization; and (iv) differential ^{13}C line widths and T_1 values which are related to the different motions in crystalline and noncrystalline esters.

REFERENCES

Adebodun, F., Chung, J., Montez, B., Oldfield, E., & Shan, X. (1992) *Biochemistry 31*, 4502–4509.

Barall, E. M., II, & Johnson, J. F. (1974) in *Liquid Crystals and Plastic Crystals* (Gray, G. W., & Winsor, P. A., Ed.) Vol. 2, pp 254–306, Ellis Horwood Limited, New York.

Bociek, S. M., Ablett, S., & Norton, I. T. (1985) *J. Am. Oil Chem. Soc. 62*, 1261–1266.

Bovey, F. A. (1988) *Nuclear Magnetic Resonance Spectroscopy* (Bovey, F. A., Jelinski, L., & Mirau, P. A., Ed.) Academic Press, Inc., New York.

Brown, M. S., & Goldstein, J. L. (1986) *Science 232*, 34–47.

Byrn, S. R., Sutton, P. A., Tobias, B., Frye, J., & Main, P. (1988) *J. Am. Chem. Soc. 110*, 1609–1614.

Croll, D. H., Small, D. M., & Hamilton, J. A. (1985) *Biochemistry 24*, 7971.

Croll, D. H., Small, D. M., & Hamilton, J. A. (1986) *J. Chem. Phys. 85*, 7380–7387.

Crvaen, B. M. (1986) *The Physical Chemistry of Lipids, From Alkanes to Phospholipids* (Small, D. M., Ed.) Chapter 6, Plenum press, New York.

Craven, B. M., & Guerina, N. G. (1979) *Chem. Phys. Lipids 24*, 91–98.

Dahlen, B. (1979) *Chem. Phys. Lipids 23*, 179–188.

Davis, G. J., Porter, R. S., & Barrall, E. M. (1970) *Mol. Cryst. Liq. Cryst. 10*, 1–19.

Dorset, D. L. (1985) *J. Lipid Res. 26*, 1142–1150.

Fyfe, C. A. (1983) *Solid State NMR for Chemistry* (Fyfe, C. A., Ed.) Chapter 7, CFC Press, Ontario, Canada.

Forbes, J., Bowers, J., Shan, X., Moran, L., & Oldfield, E. (1988a) *J. Chem. Soc., Faraday Trans. I 84*, 3821–3849.

Forbes, J., Husted, C., & Oldfield, E. (1988b) *J. Am. Chem. Soc. 110*, 1059–1065.

Gao, Q., & Craven, B. M. (1986) *J. Lipid Res. 27*, 1214–1221.

Ginsburg, G. S., & Small, D. M. (1981) *Biophys. Biochim. Acta 664*, 98.

Ginsburg, G. S., Small, D. M., & Hamilton, J. A. (1982) *Biochemistry 21*, 6857–6867.

Ginsburg, G. S., Atkinson, D., & Small, D. M. (1984) *Prog. Lipid Res. 23*, 135–1647.

Gorrissen, H., Tulloch, A. P., & Cushley, R. (1980) *Biochemistry 19*, 3422–3429.

Gray, G. W. (1962) *Molecular Structure and Properties of Liquid Crystals*, pp 1–314, Academic Press, New York.

Griffin, R. G. (1981) *Methods Enzymol. 72*, 108–174.

Hamilton, J. A., & Small, D. M. (1982) *J. Biol. Chem. 257*, 7318–7321.

Hamilton, J. A., Oppenheimer, N., & Cordes, E. H. (1977) *J. Biol. Chem. 252*, 8071–8080.

Hamilton, J. A., Miller, K. W., & Small, D. M. (1983) *J. Biol. Chem. 258*, 12821–12826.

Jacobs, R. E., & Oldfield, E. (1981) *Progr. Nucl. Magn. Reson. Spectrosc. 14*, 113–136.

Jones, A., & Glomset, J. (1985) *Sterols and Bile Acids* (Danielsson, H., & Sjovall, J., Eds.) pp 95–119, Elsevier Science Publishers, New York.

Kroon, P. A. (1981) *J. Biol. Chem. 256*, 5332–5339.

Lafontaine, E., Bayle, J. P., & Courtieu, J. (1989) *J. Am. Chem. Soc. 111*, 8294–8926.

Luz, Z., Poupko, R., & Samulski, E. T. (1981) *J. Chem. Phys. 74*, 5825–5836.

Moller, M., Gronski, W., Cantow, H.-J., & Hocker, H. (1984) *J. Am. Chem. Soc. 106*, 5093–5099.

Norton, I. T., Lee-Tuffnell, C. D., Ablett, S., & Bociek, S. M. (1985) *J. Am. Oil Chem. Soc. 62*, 1237–1244.

Oldfield, E., Bowers, J. L., & Forbes, J. (1987) *Biochemistry 26*, 6919–6923.

Oldfield, E., Adebodun, F., Chung, J., Montez, B., Park, K. D., Le, H.-B., Philips, B. (1991) *Biochemistry 30*, 11025–11028.

Opella, S. J. & Frey, M. H. (1979) *J. Am. Chem. Soc. 101*, 5854–5856.

Rothwell, W. P., & Waugh, J. S. (1981) *J. Chem. Phys. 74*, 2721–2732.

Small, D. M. (1970) in *Surface Chemistry of Biological Systems* (Blank, M., Ed.) p 55–83, Plenum Publishing Co., New York.

Small, D. M. (1988) *Arteriosclerosis 8*, 103–129.

Smith, S. O., Palings, I., Copie, V., Raleigh, D. P., Courtin, J., Pardoen, J. A., Lugtenburg, J. Mathies, R. A., & Griffin, R. G. (1987) *Biochemistry 26*, 1606–1611.

Snow, J. W., & Phillips, M. C. (1990) *Biochemistry 29*, 2464–2471.

Snow, J. W., Glick, J. M., & Phillips, M. C. (1992) *J. Biol. Chem. 267*, 18564–18572.

Suwelack, D., Rothwell, W. P., & Waugh, J. S. (1980) *J. Chem. Phys. 73*, 2559–2569.

Torchia, D. A. (1978) *J. Magn. Reson. 30*, 613–616.

VanderHart, D. L., Earl, W. L., & Garroway, A. N. (1981) *J. Magn. Reson. 44*, 361–401.

Webb, G. G., & Zilm, K. W. (1989) *J. Am. Chem. Soc. 111*, 2455–2463.